



## Shallow remineralization in the Weddell Gyre

**Regina Usbeck and Michiel Rutgers van der Loeff**

*Alfred Wegener Institute for Polar and Marine Research, P.O. Box 120161, 27515 Bremerhaven, Germany  
(rusbeck@awi-bremerhaven.de; mloeff@planet.nl)*

**Mario Hoppema**

*University of Bremen, Institute of Environmental Physics, Department of Oceanography, P.O. Box 330440, 28334 Bremen, Germany (hoppema@theo.physik.uni-bremen.de)*

**Reiner Schlitzer**

*Alfred Wegener Institute for Polar and Marine Research, P.O. Box 120161, 27515 Bremerhaven, Germany  
(rschlitzer@awi-bremerhaven.de)*

[1] The region influenced by the Polar Front in the Southern Ocean is characterized by relatively high productivity, which is mirrored in strong depletions of  $^{234}\text{Th}$  in the surface water, a good tracer of export production, and by high accumulation rates on the underlying seabed. Farther south, the Weddell Sea is generally considered a low productivity region with very low export fluxes. This finding is based on satellite observations, sediment accumulation rates, trap deployments, and phytoplankton distribution. If this would be true,  $^{234}\text{Th}$  should be close to equilibrium with its parent. However, in a series of high-resolution transects of  $^{234}\text{Th}/^{238}\text{U}$  across the Antarctic Circumpolar Current (ACC),  $^{234}\text{Th}$  was found to be depleted by 10–15% throughout the clear Weddell Gyre, only to reach equilibrium in sea-ice covered regions of the coastal zone. Vertical profiles showed that the depletion was limited to the upper mixed layer and was balanced by an enrichment of similar magnitude at 100–250m depth. This implies that the export of particles below 250 m is negligible. Such shallow remineralization is in line with the discrepancies between biogenic silica production rates and sediment trap data observed in the Weddell and Ross Seas. These observations in the Weddell Sea are fully consistent with our inverse modeling results for both organic carbon and opal, and they are not inconsistent with  $\text{TCO}_2$  and oxygen sections that show a  $\text{TCO}_2$  enriched, oxygen reduced shallow subsurface layer. This blue ocean, characterized by upwelling of  $\text{CO}_2$ -enriched deep waters, supports sufficient productivity to be a net sink for  $\text{CO}_2$  to abyssal depths [Hoppema *et al.*, 1999]. No record of this productivity and export is stored in the underlying sediment, which has important palaeoceanographic consequences.

**Components:** 8504 words, 14 figures.

**Keywords:** Weddell Gyre; export; remineralization; Thorium-234; carbon; silica.

**Index Terms:** Geochemical cycles; Marine Geochemistry; Biogeochemical processes; Arctic and Antarctic oceanography.

**Received** 17 May 2001; **Revised** 17 October 2001; **Accepted** 18 October 2001; **Published** 31 January 2002.

R. Usbeck, M. M. Rutgers van der Loeff, M. Hoppema, and R. Schlitzer, Shallow remineralization in the Weddell Gyre, *Geochem. Geophys. Geosyst.*, 3(1), 10.1029/2001GC000182, 2002.

## 1. Introduction

[2] Upwelling of Circumpolar Deep Water in the Southern Ocean brings old, nutrient and CO<sub>2</sub>-enriched deep waters in contact with the atmosphere. The balance of this physical pump (upwelling) and the biological pump (export production) in the Southern Ocean is considered to be a key issue in the coupling of ocean circulation to atmosphere and climate. It has been suggested that increased export production during glacials was a major reason of the glacial CO<sub>2</sub> drawdown [Sarmiento and Toggweiler, 1992] and may have been caused by enhanced iron inputs [Martin and Gordon, 1988; Anderson et al., 1998], but others maintain that it was rather the reduced physical pump by the more extensive ice cover and more effective stratification that caused the change in air-sea exchange [Francois et al., 1997; Veizer et al., 2000; Stephens and Keeling, 2000]. If we want to understand what controls the air-sea exchange in the Southern Ocean, it is important to know and understand the present fluxes. Today the Weddell Gyre appears to be a sink for atmospheric CO<sub>2</sub> [Hoppema et al., 1999; Stoll et al., 1999], but in earlier days, this has probably not been the case. The regional distribution of present export production in the Southern Ocean has been estimated from satellite data, from compilations of water column data, and from compilations of the recent sedimentary record.

[3] The most conspicuous element of the sedimentary record in the Southern Ocean is the Opal Belt, showing very high accumulation rates and consequently export production of biogenic silica in a zone of 5–10° of latitude south of the Antarctic Polar Front, in the southern Atlantic corresponding to the zone of ~50–55°S [Lisitzin, 1996; DeMaster, 1981]. Farther south, in the Weddell Gyre, sediment accumulation rates are negligibly small. Benthic fluxes as determined from oxygen and nutrient pore water profiles [Schlüter et al., 1998] confirmed the low rain rates compared to other ocean basins (e.g., compiled by Jahnke [1996]), whereas the low inventories of <sup>210</sup>Pb [Rutgers van der Loeff and Berger, 1993] and of <sup>230</sup>Th and <sup>231</sup>Pa [Walter et al., 2001] completed the picture of extremely low flux rates in the water column of the central Weddell Sea.

When the first sediment trap results from the Weddell Gyre appeared [Fischer et al., 1988] with the lowest fluxes ever observed (at a depth of 700 m), the situation appeared clear: The Weddell Sea (with the exception of the coastal zone and the upwelling- and polynya-affected area around Maud Rise) was considered an ocean desert. Even the clearly higher particle flux collected later at the sediment trap AWI 208 in the central Weddell Sea [Walter et al., 2000] still agreed with the relatively low particle rain rate in the central Weddell Sea. However, the ratio of opal burial to opal production turned out to be very much lower in the Weddell Sea than in the ACC [Leynaert et al., 1991, 1993; Schlüter et al., 1998]. Production rates of biogenic silica determined by Leynaert et al. [1993] in the central/northern Weddell Sea, which were indeed relatively low compared with estimates from the ACC, were 2 orders of magnitude higher than the opal flux reported from the traps at 700 m depth. These authors hypothesized an efficient remineralization in the upper few hundred meters of the ocean to bring their results in agreement with the other published data. Pondaven et al. [2000] found that the opal preservation in the Southern Ocean (Indian Sector) was substantially lower than previously thought and attributed this to a former underestimation of opal production rates as well as to an overestimation of opal burial rates. Similar indications were obtained with regard to the flux of organic material.

[4] The Central Intermediate Water in the central Weddell Sea rises to a depth of ~400 m and is characterized by low oxygen and high nutrient contents as a result of in situ remineralization [Whitworth and Nowlin, 1987]. These signs of shallow remineralization were confirmed by high-resolution transects of TCO<sub>2</sub> and O<sub>2</sub> [Hoppema et al., 1997]. The maps of Berger [1989] compiled in part based on phosphate data also show considerable amounts of primary production and export production of organic carbon south of the ACC. These results imply that the export flux from the surface water is higher than the geological record or even the results of sediment traps had suggested. The 8-year-long record of the Coastal Zone Color Scanner (CZCS) satellite images and the accumulating record of Sea-viewing Wide Field-of-view

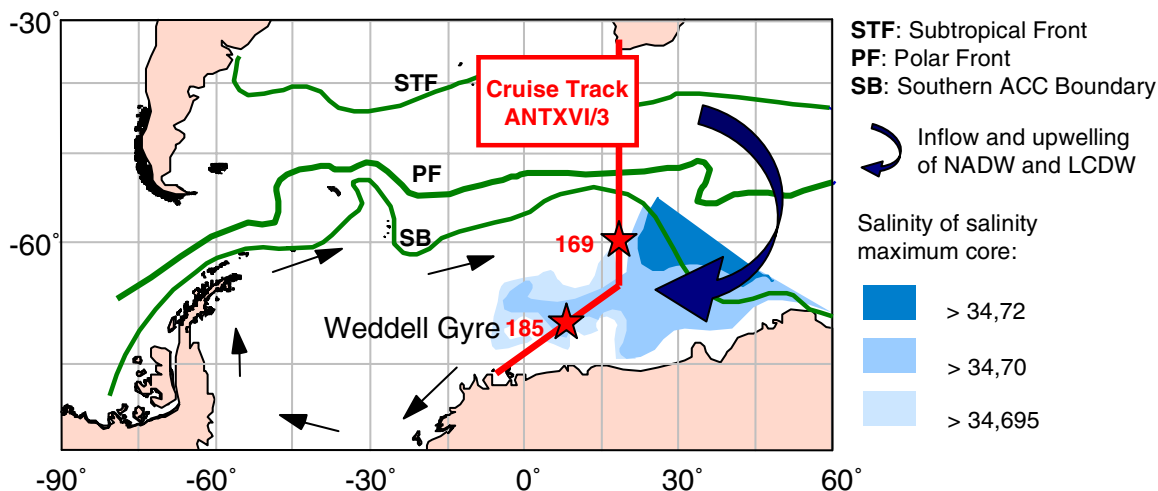


**Figure 1.** The Weddell Gyre and the frontal system in the Atlantic. Fronts are drawn according to Orsi *et al.* [1995], salinity of salinity maximum core are after Orsi *et al.* [1993] (redrawn from Geibert [2001]).

Sensor (SeaWiFS) pictures show the distribution of chlorophyll in the surface water and therefore give an impression of the distribution of primary production. The data suggest the ACC and especially the area downstream of Drake Passage and the tip of the Antarctic Peninsula to be productive areas. The data coverage south of the ACC deteriorates with latitude due to cloud cover, ice, and light conditions, but the area is generally low in chlorophyll. Nevertheless there are recurring blooms even in this zone, like in January 1998 in the central Weddell Sea (SeaWiFS data available at <http://seawifs.gsfc.nasa.gov/SEAWIFS.html>).

[5] In this paper we try to reconcile the opposing indications of negligible sediment accumulation and low fluxes in the water column at middepth on the one hand with the occasional blooms and generally appreciable fluxes in the upper water column on the other. We present evidence based on the distribution of nutrients,  $\text{TCO}_2$ , dissolved oxygen, and  $^{234}\text{Th}$  for unusually shallow remineralization in the eastern Weddell Gyre and discuss the consequences for the role of the Antarctic Zone of the Southern Ocean in the global carbon cycle.

## 2. Hydrography, $\text{TCO}_2$ , and Oxygen

[6] In our area of investigation, two main oceanic provinces are distinguished, the Antarctic Circum-

polar Current in the north and the subpolar Weddell Gyre in the south. The boundary between them is characterized by a sharp front, called ACC-Weddell Gyre boundary or Weddell Front, which at the prime meridian occurs at  $\sim 55^\circ\text{S}$  [Orsi *et al.*, 1995; Schröder and Fahrbach, 1999]. The huge eastward ACC water transport is concentrated in some frontal jets, in particular the Subantarctic Front (SAF), the Polar Front (PF), and the Southern ACC Front [Orsi *et al.*, 1995]. Though the flow direction of the ACC is predominantly zonal, also a significant southward flow component exists. As part of this, the Circumpolar Deep Water (CDW), the most voluminous subsurface water mass of the ACC, shoals considerably to the south. In the southernmost ACC south of the PF, the Upper CDW is entrained into the surface layer. Upon meeting the southern boundary of the ACC, the Lower CDW is trapped into the Weddell Gyre near its eastern edge [Deacon, 1979], thence constituting the intermediate water and a major subsurface water supply of the Weddell Gyre. The Weddell Gyre is a large elongated cyclonic feature (Figure 1), which transports  $\sim 60$  Sv of water essentially in a marginal current [Schröder and Fahrbach, 1999; Beckmann *et al.*, 1999]. In its southern limb, water at almost all depths flows westward. This includes the recently injected CDW (Figure 2), which is locally called Warm

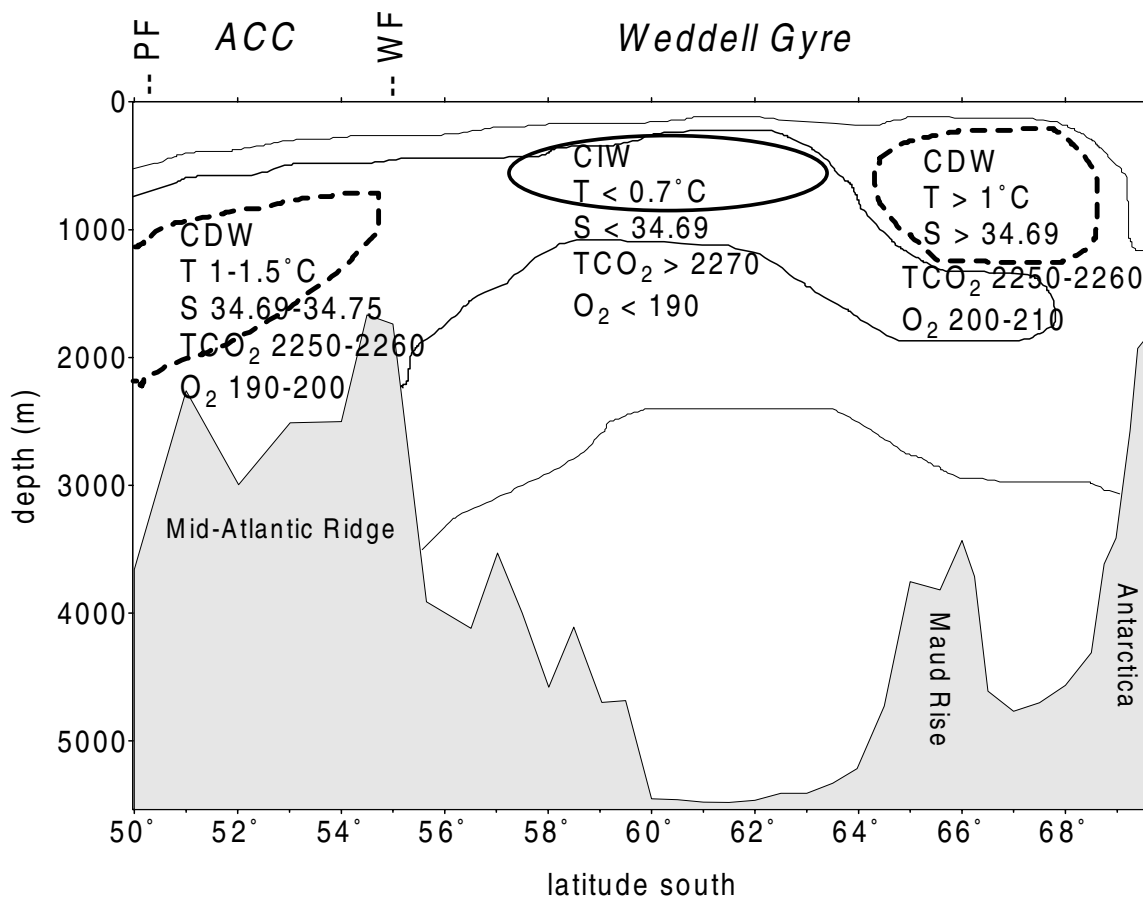


**Figure 2.** Schematic representation of a section across the Antarctic Circumpolar Current (ACC) and Weddell Gyre at the prime meridian for illustrating the locations of the Circumpolar Deep Water (CDW) and the Central Intermediate Water (CIW). Typical values for potential temperature ( $T$ ), salinity ( $S$ ), and the concentrations of  $\text{TCO}_2$  and oxygen (both in  $\mu\text{mol/kg}$ ) are indicated, based on data of *Hoppema et al.* [1997] and *Schröder and Fahrbach* [1999]. PF, Polar Front; WF, Weddell Front.

Deep Water (WDW). From the Antarctic Peninsula on, the northern limb carries the return flow to the east. Figure 2 shows a cartoon of a vertical section through the southern ACC and the Weddell Gyre. Indicated are typical ranges of temperature, salinity,  $\text{TCO}_2$ , and oxygen [*Whitworth and Nowlin*, 1987; *Hoppema et al.*, 1997; *Schröder and Fahrbach*, 1999]. Within the Weddell Gyre, the subsurface layer is characterized by maxima of temperature, salinity, and  $\text{TCO}_2$  (and nutrients) and a minimum of oxygen. The maxima are initially induced by the entrainment of deep water from the ACC into the Weddell Gyre water column, where both the surface water and the deep water of the gyre have a relatively low-temperature, salinity, and  $\text{TCO}_2$  concentration. For

oxygen, exactly the opposite holds. From Figure 2 it is evident that the deeper water masses in the ACC possess essentially the same properties as the subsurface water mass in the southern Weddell Gyre.

[7] During its flow path through the gyre, the CDW gets fresher and colder through mixing with water above and below [*Fahrbach et al.*, 1994]: In the northern limb of the gyre, which is situated downstream within the gyre circulation, temperature and salinity are significantly lower in the temperature maximum/salinity maximum layer. Mixing with water above and below would also decrease  $\text{TCO}_2$  but increase oxygen, because the surface and deep water have relatively low  $\text{TCO}_2$ /high oxygen concentrations. However, instead of

that, a higher  $\text{TCO}_2$ /lower oxygen concentration is found [Whitworth and Nowlin, 1987; Hoppema *et al.*, 1997]. This layer with elevated  $\text{TCO}_2$ /reduced oxygen is predominantly found in the central part of the gyre; it has been termed Central Intermediate Water (CIW) by Whitworth and Nowlin [1987]. Because the CDW is essentially the only supply of intermediate water of the Weddell Gyre, this  $\text{CO}_2$  enrichment /oxygen decrease can only be generated locally. The only process that could produce  $\text{CO}_2$  and consume oxygen is degradation of organic matter. Elevated  $\text{TCO}_2$ /reduced oxygen values occur in the subsurface layer approximately between 200 and 700 m depth. Thus the hydrographical and  $\text{TCO}_2$ /oxygen sections give a first indication for shallow remineralization in the central Weddell Sea.

### 3. Methods

#### 3.1 Thorium

[8] The  $^{234}\text{Th}$  was measured in surface waters on N-S transects during the “Polarstern” expedition ANT XVI/3 (March–April 1999 [Bathmann *et al.*, 2000]) as a means to map the latitudinal distribution of export production. The activity in profiles sampled with the Rosette sampler was measured in order to quantify the cumulative depletion and to estimate the export flux. The method used for  $^{234}\text{Th}$  followed Rutgers van der Loeff and Moore [1999]. This method requires a sample volume of  $\sim 20$  L. During the expedition, an alternative procedure was developed allowing the quantification of total  $^{234}\text{Th}$  on 5 L samples with appreciably less manipulation. Briefly, to 5 L of seawater are added 125  $\mu\text{L}$  of a  $\text{KMnO}_4$  solution (60 g/L) and two drops of ammonia. After mixing, 200  $\mu\text{L}$  of  $\text{MnCl}_2$  solution are added (40 g  $\text{MnCl}_2 \times \text{H}_2\text{O/L}$ ). The sample is mixed and allowed to stand for at least 1 hour. The sample is then passed by pressure filtration (50 kPa) over a 25-mm graded glass fiber filter (1  $\mu\text{m}$  pore size). The volume of the filtrate is determined by weighing. The filter is rinsed with demineralized water, dried, and beta counted. For more details see Benitez-Nelson *et al.* [2001]. All analyses and counting were done on board ship. Deep water samples of  $^{234}\text{Th}$  ( $>500$  m depth;  $>500$  m above seafloor) are used for

calibration, assuming equilibrium with  $^{238}\text{U}$ . As we were highly surprised by the consistent 15% depletion of total  $^{234}\text{Th}$  in the clear surface water of the Weddell Sea, we double-checked this by collecting 20 L filtered samples in triplicate, acidified them with 1 mL/L of 6M HCl, stored them for seven half lives, and analyzed them after neutralization with ammonia with the same  $\text{MnO}_2$  precipitation technique and the same standards in the home laboratory (Figure 3). All samples had grown to equilibrium, proving that the depletion in the surface water of the Weddell Sea was real.

#### 3.2 Inverse Modeling

[9] The global circulation field together with parameters for biogenic particle fluxes was investigated using the AWI Adjoint Model for Oceanic Carbon Cycling (AAMOCC). The model was originally developed by Schlitzer [1993] to calculate the ocean circulation, air-sea fluxes of heat and fresh water, and mixing coefficients in the Atlantic. The basic concept of the model is to use the information stored in distributions of temperature and salinity to drive ocean circulation. Ocean currents are calculated inversely to reproduce long-term average hydrographic data. The model conserves mass, heat, salt, and tracers and the resulting flow field fulfills the geostrophic principle. The model determines mean velocities together with air-sea heat and fresh water fluxes and mixing coefficients, which give distributions close to data. The model was expanded by de las Heras and Schlitzer [1999] to a global domain. The model grid is nonuniform with a basic grid cell of  $2^\circ$ – $4^\circ$  in latitude and  $2.5^\circ$ – $5^\circ$  in longitude. Important areas and areas with strong gradients as the Antarctic Polar Front are better resolved, whereas the big ocean basins are mostly covered with grid cells  $4^\circ \times 5^\circ$  (latitude  $\times$  longitude). The vertical resolution decreases from  $\sim 60$  m at the surface to  $\sim 500$  m at the deepest layers. Schlitzer [2000] included the possibility to determine vertical biogenic particle fluxes from data of dissolved nutrients. The exact satisfaction of budget equations allows the computation of cycles of phosphate, nitrate, and silicate: For a stationary, mean ocean circulation, the transport of nutrients due to

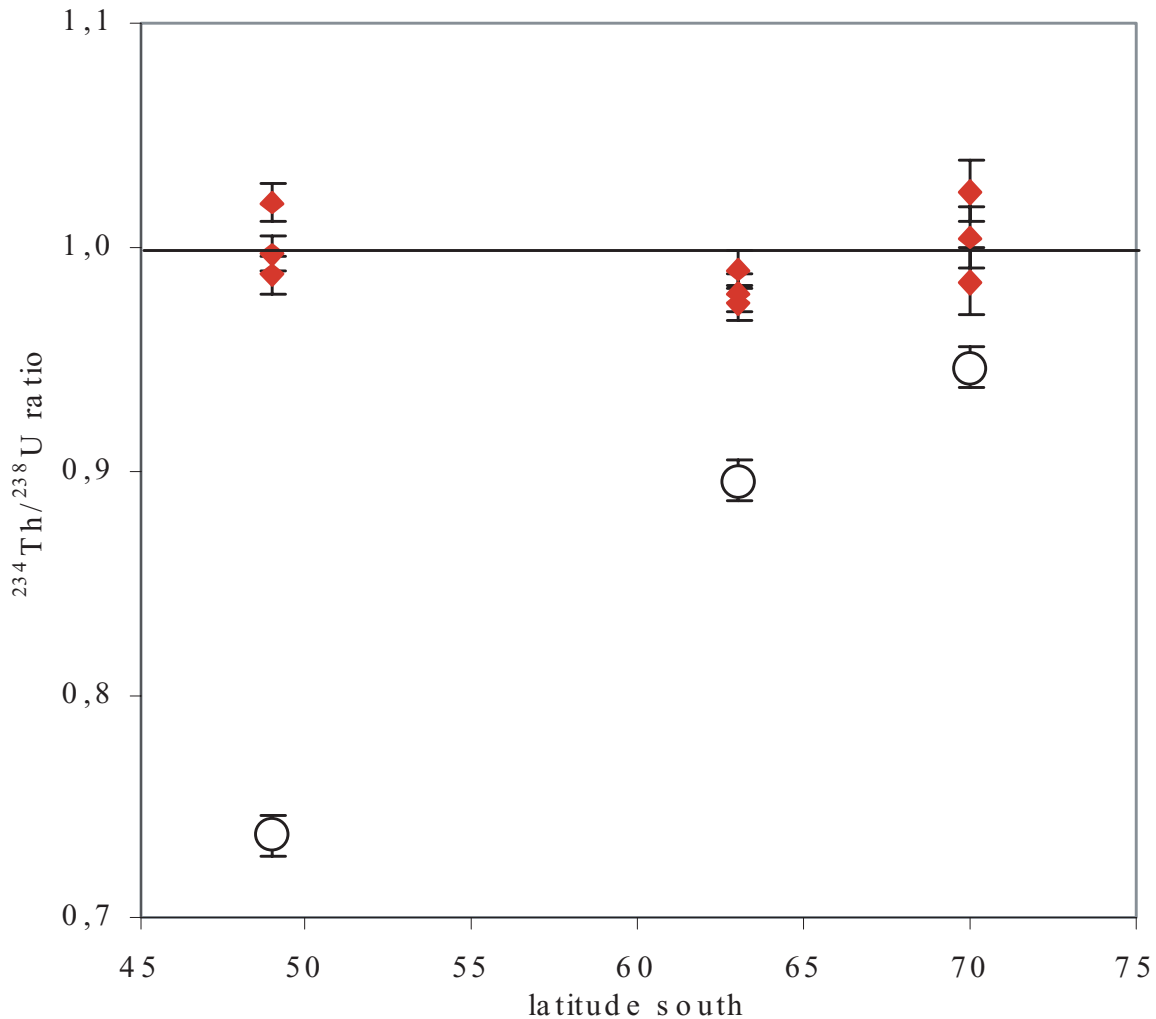


**Figure 3.** Ingrowth of  $^{234}\text{Th}$  (total  $^{234}\text{Th}$  with 1-sigma counting errors) from in situ values (open symbols) to equilibrium (after 7 half lives, closed symbols) with  $^{238}\text{U}$  in surface water samples as a function of latitude confirming the calibration procedure.

advection and diffusion processes must be in equilibrium with vertical particle fluxes. In principle, nutrients brought to the euphotic zone by upwelling are used for particle formation which results in a sink of dissolved nutrients in the corresponding model boxes. Sinking particles, which are remineralized, serve as a nutrient source in the boxes of the underlying water column. Calculating the mean advective/diffusive transports of nutrients and the comparison with data of dissolved nutrients yields the sources and sinks of dissolved nutrients in the whole water column which are virtually explained by particle formation in surface waters and remineralization below. Particle fluxes  $J$  are calculated using Suess-type

functions of the form  $J \sim a \times z^{-b}$  [Suess, 1980]. The parameters  $a$  and  $b$  are regionally variable and optimized by the model for organic carbon and opal separately: Organic carbon is controlled by nutrient budgets of phosphate, nitrate, total carbon, and oxygen with constant Redfield ratios [Redfield *et al.*, 1963]; opal fluxes are controlled by budgets of dissolved silicate.

[10] A typical model run is performed as follows (cf. Figure 4):

1. Initial values for all parameters are applied for the whole model grid. Model parameters are horizontal velocities, mixing coefficients, surface heat and fresh water fluxes, surface gas ex-

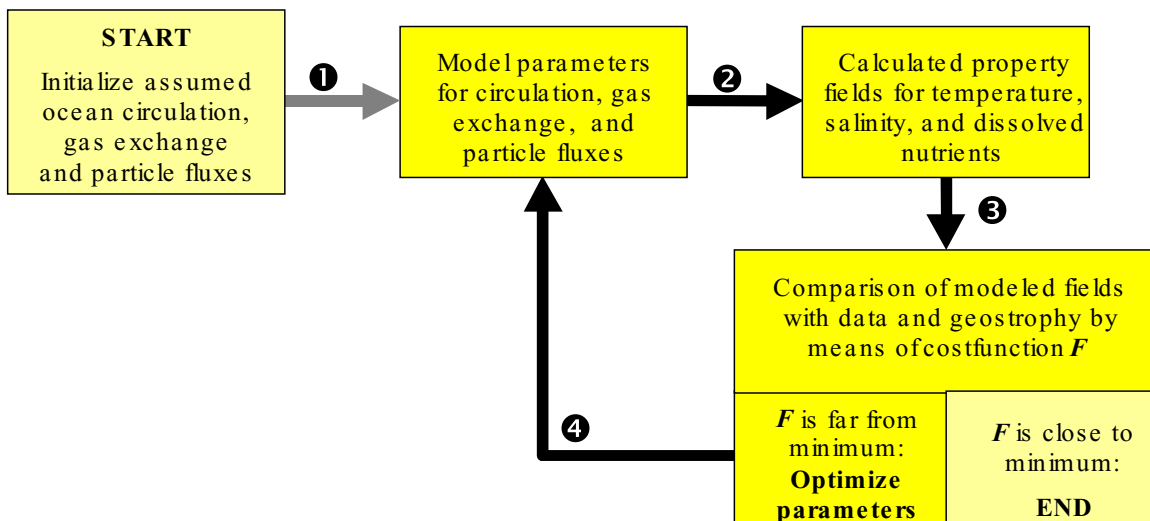
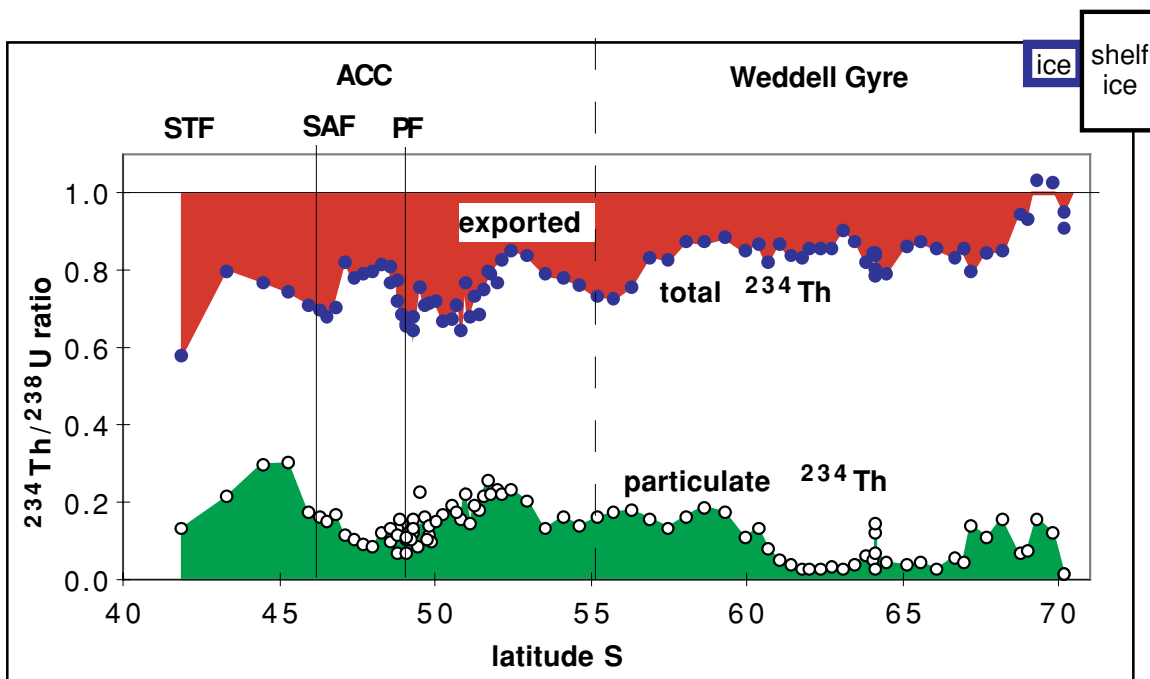


Figure 4. Sketch of the concept of the AAMOCC model.

change rates, export production, remineralization rates and accumulation rates of biogenous particulate matter.

2. A linear system  $A \times c = q$  is solved for all properties of interest. Here  $A$  is the

advection/diffusion matrix,  $c$  is the concentration vector of the property of interest, and  $q$  is the respective source term. This yields property distributions for temperature, salinity, and dissolved nutrients.



ANT XVI/3, March-April 1999

Figure 5. Particulate (open symbols) and total (particulate + dissolved, closed symbols)  $^{234}\text{Th}$ , expressed as ratio to its parent  $^{238}\text{U}$ , in surface water as function of latitude on the North-South transects, showing strongest depletion near the Subtropical (STF), Subantarctic (SAF), and south of the Polar Front (PF), and very low particulate levels in the Weddell Gyre.

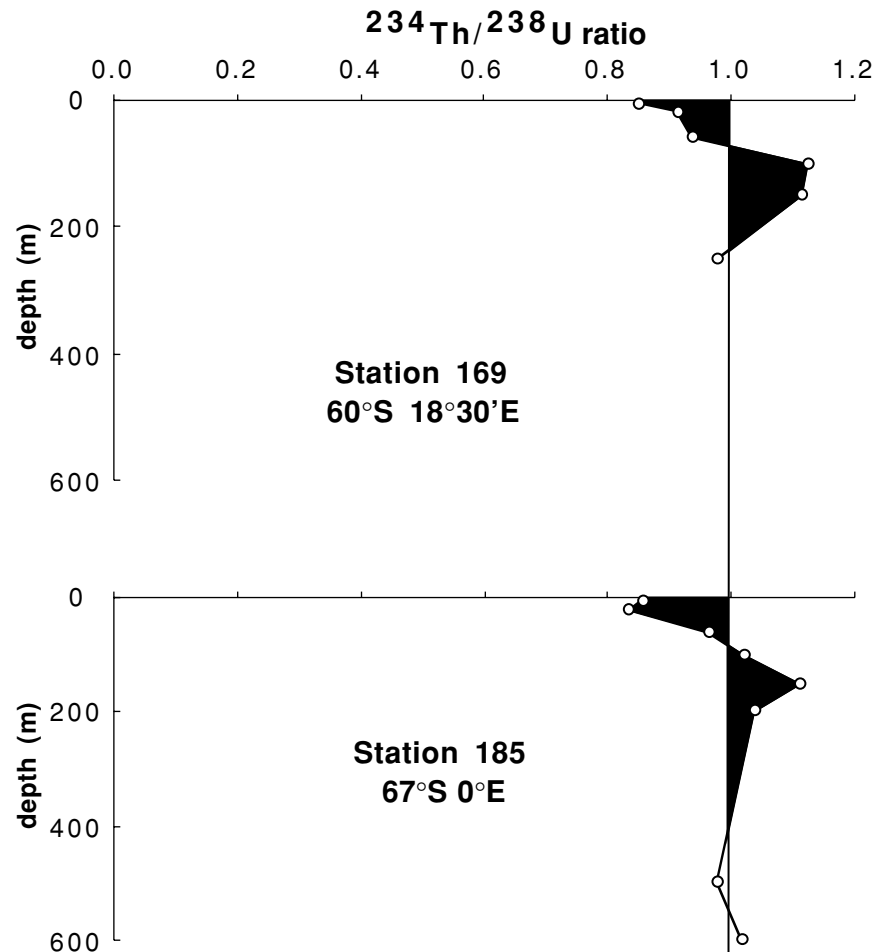


**Figure 6.** Depth profiles of total  $^{234}\text{Th}/^{238}\text{U}$  activity ratio, showing remineralization maxima below the pycnocline in the central Weddell Sea.

3. The resulting property fields are automatically compared to measurements, and model-data misfits are accumulated in a cost function  $F$ . Additionally,  $F$  contains penalty terms for deviations from initial geostrophic shear values and smoothness constraints. All terms in  $F$  are multiplied by weight factors allowing to align the individual terms for special demands. The cost function is a scalar function which measures the quality of the model solution: a smaller cost function indicates that the model solution better complies with data of temperature, salinity, and dissolved nutrients, while the flow field complies with the geostrophic principle.

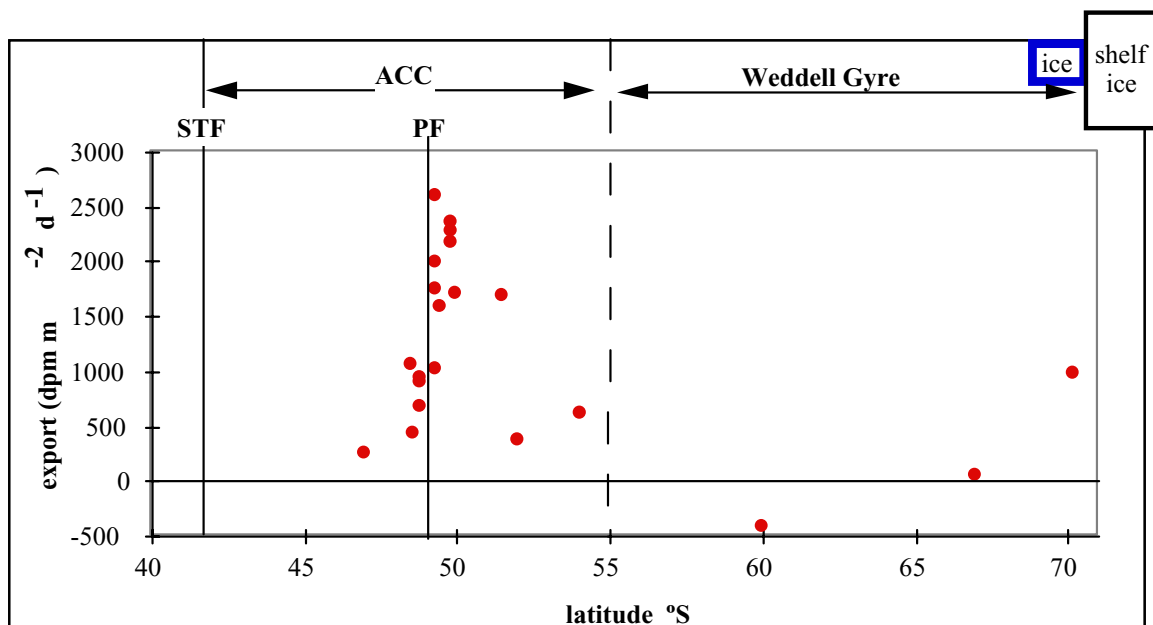
4. If the cost function is at or near minimum, the iteration is terminated. Otherwise, the cost function  $F$  is minimized with respect to the model parameters and the model reiterates.

[11] A more detailed description of the AAMOC model is given in *Schlitzer* [1993, 1995, 2000], *de las Heras and Schlitzer* [1999], and *Usbeck* [1999]. The original data set used in the adjoint formalism contains more than 25,000 worldwide stations of historical hydrographic and nutrient data [Schlitzer, 2000]. The data from *Hoppema et al.* [1997] discussed above were not included in the calculations.

## 4. Results

### 4.1. Geographical Distribution of $^{234}\text{Th}$ Depletion

[12] The latitudinal distribution of particulate and total  $^{234}\text{Th}$  in surface waters in March 1999, expressed as activity ratio to the parent  $^{238}\text{U}$ ,



ANT XVI/3, March-April 1999

**Figure 7.** Steady state export flux of  $^{234}\text{Th}$  from the upper 200 m, based on depth-integrated depletion relative to  $^{238}\text{U}$ , versus latitude.

shows distinct export signals which appear to be linked to the position of the ACC fronts and large areas with little export (Figure 5). Highest depletion was observed around  $42^\circ\text{S}$  near the Subtropical Front, around  $46^\circ\text{S}$  near the Subantarctic Front, just south of the Polar Front around  $50^\circ\text{S}$ , and in a wider zone around  $55^\circ\text{S}$  which may correspond to the ACC/Weddell Gyre boundary. The Polar Front Zone (PFZ) had a relatively low depletion, showing that this zone had not given rise to appreciable export production in the preceding 1–2 months. The Weddell Gyre was characterized by extremely low particle contents, reflected in low particulate  $^{234}\text{Th}$  activities ( $61^\circ\text{S}$ – $67^\circ\text{S}$ ). Nevertheless a depletion of  $\sim 15\%$  in total  $^{234}\text{Th}$  was observed throughout the Gyre. Only close to the Antarctic continent, in the sea ice-covered coastal zone,  $^{234}\text{Th}$  activities reached equilibrium with  $^{238}\text{U}$ .

#### 4.2. Vertical Distribution of $^{234}\text{Th}$

[13] The vertical distribution of total  $^{234}\text{Th}$  was determined in order to derive the cumulative deple-

tion relative to its parent  $^{238}\text{U}$ . Near the Polar Front the profiles showed a strong depletion in the upper 100–150 m. A remarkable result of some profiles is significant  $^{234}\text{Th}$  excess below the pycnocline. In the Weddell Gyre, the depletion of  $\sim 15\%$  in the surface water is limited to a shallow layer of just  $\sim 100$  m. This depletion is about balanced by the integrated excess in the depth zone 100–250 m (Figure 6), indicating very little export to deeper layers (see section 4.3).

#### 4.3. Thorium Derived Export Fluxes

[14] If the depletion changes with time, the export flux of  $^{234}\text{Th}$  has to be calculated according to the nonsteady state model of Buesseler *et al.* [1992]. Some stations were visited 2 or 3 times over a period of 5 weeks. The depth distribution at  $49^\circ\text{S}$ – $50^\circ\text{S}$  (not shown) changed somewhat toward a lower depletion at the surface and a higher depletion at 100 m depth, but the integrated depletion remained the same. This can be explained by the deepening of the mixed layer (V. Strass, personal communication, 2001). As the cumulative depletion

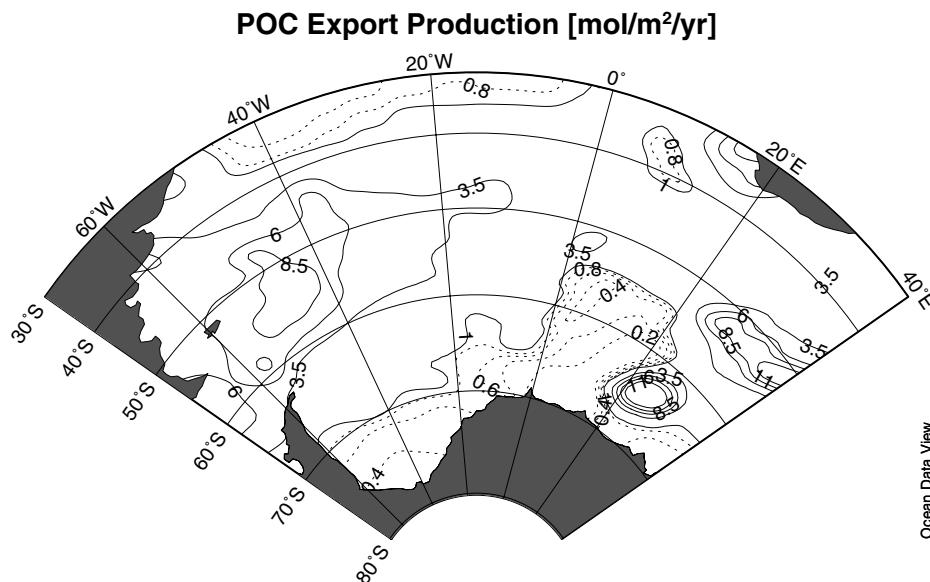


**Figure 8.** Annual POC export production at 133 m depth from the AAMOC model.

remained constant in time over 1 month or more than the half-life of  $^{234}\text{Th}$ , we can assume steady state here. The corresponding estimate of export fluxes at 200 m depth at all stations (Figure 7) shows that highest export fluxes occur just south of the Polar Front. Further south, export fluxes at 350 m depth are negligible in the open Weddell Gyre.

#### 4.4. Inverse Modeling

[15] The circulation field derived with the adjoint model in the present study is similar to the flow field presented by *de las Heras and Schlitzer* [1999] and contains all major currents. The Weddell Gyre turns southward between  $10^\circ$  and  $30^\circ\text{E}$ , and the upwelling of CDW predominantly occurs east of Maud Rise. At a global scale, simulated particulate organic carbon fluxes are realistic with high export fluxes along the eastern margins of the ocean basins and near the Antarctic Polar Frontal system. Model opal fluxes are high in the North Pacific and the Antarctic. Integrated fluxes of organic carbon are within the range of independent estimates by different models [*Schlitzer*, 2000; *Yamanaka and Tajika*, 1996, 1997; *Najjar et al.*, 1992]. Global model opal fluxes at 133 m depth are  $\sim 25\%$  higher than *Nelson et al.*'s [1995] estimate at 200 m. Model data misfits of hydrographic and dissolved nutrient data are smaller than 10% (volume weighted mean).

#### 4.5. POC Fluxes

[16] South of  $30^\circ\text{S}$ , model export fluxes of organic carbon are highest in a band around Antarctica; the geographical distribution is quite similar to *Berger's* [1989] map of primary production. In the Atlantic, high organic carbon fluxes are found in and east of Drake Passage and in the Argentine Basin (Figure 8). Toward the east, fluxes decrease, but south of Africa, at  $\sim 30^\circ\text{E}$ , fluxes increase again reaching  $\sim 2.5 \text{ mol m}^{-2}\text{yr}^{-1}$ . Organic carbon remineralization parameter  $b$  lies between 1 and 2 in most areas of the ocean. The initial value was 1 [*Suess*, 1980], and in areas with no or very low export, this value was not changed by the model. In the Weddell Sea, the parameter  $b$  is high in most areas with high export fluxes, and the geographical distribution seems to be associated with the frontal system (Figure 9). Highest remineralization rates are found around the Polar Front. The strong remineralization south of  $\sim 50^\circ\text{S}$  results in very low fluxes to the seafloor in the Weddell Gyre (Figure 10). Fluxes to the sediment larger than  $1 \text{ mol m}^{-2}\text{yr}^{-1}$  (i.e.,  $12 \text{ g C m}^{-2}\text{yr}^{-1}$ ) are, with the exception at the "hot spot" at  $65^\circ\text{S}$ ,  $25^\circ\text{E}$ , which might be an artifact in this experiment, only found in shelf areas and in the Argentine Basin. Elsewhere, fluxes larger than  $0.1 \text{ mol m}^{-2}\text{yr}^{-1}$  in

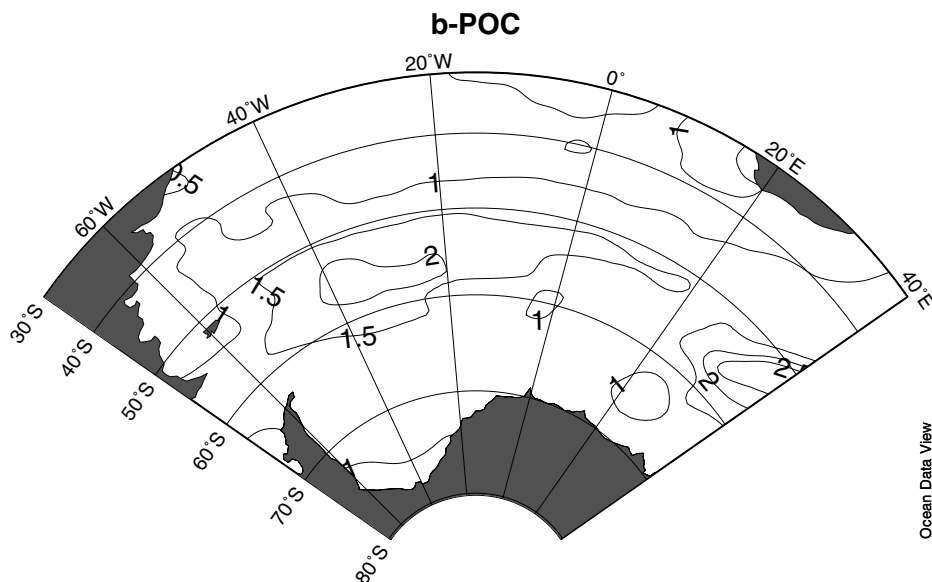


**Figure 9.** POC remineralization depth scale  $b$  from AAMOCC. Here  $b$  is the exponent in the Suess-type functions for particle flux  $a \cdot z^{-b}$ , where  $a$  is the export at 133 m depth (cf. Figure 8).

open ocean areas are restricted to a corridor around  $\sim 45^\circ\text{S}$ , i.e., north of the SAF.

#### 4.6. Opal Fluxes

[17] In the Atlantic, opal fluxes strongly increase from north to south with sharp gradients at the

Polar Front (Figure 11). High export fluxes are found east of the South Sandwich Islands and the most prominent feature is the high fluxes between  $0^\circ$  and  $30^\circ\text{E}$ , where the Weddell Gyre turns southward. Opal export in this area exceeds  $4.5 \text{ mol m}^{-2} \text{ yr}^{-1}$ , which is fairly high but in good agreement with annual silica consumption rates estimated

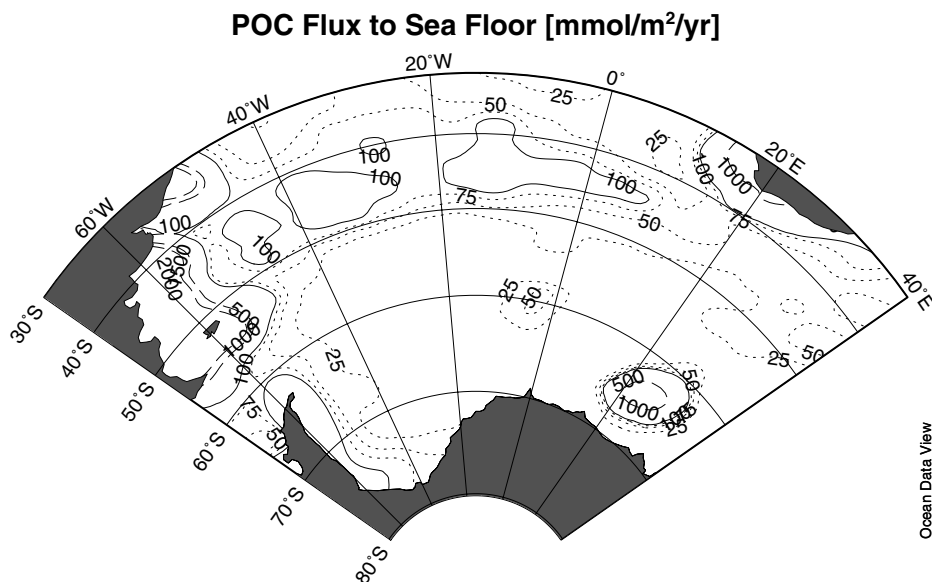


**Figure 10.** POC flux to seafloor from AAMOCC. The flux to the seafloor is given by the flux to the bottom box. From this, a part is accumulated into the surface sediments; the rest is remineralized in the bottom box.

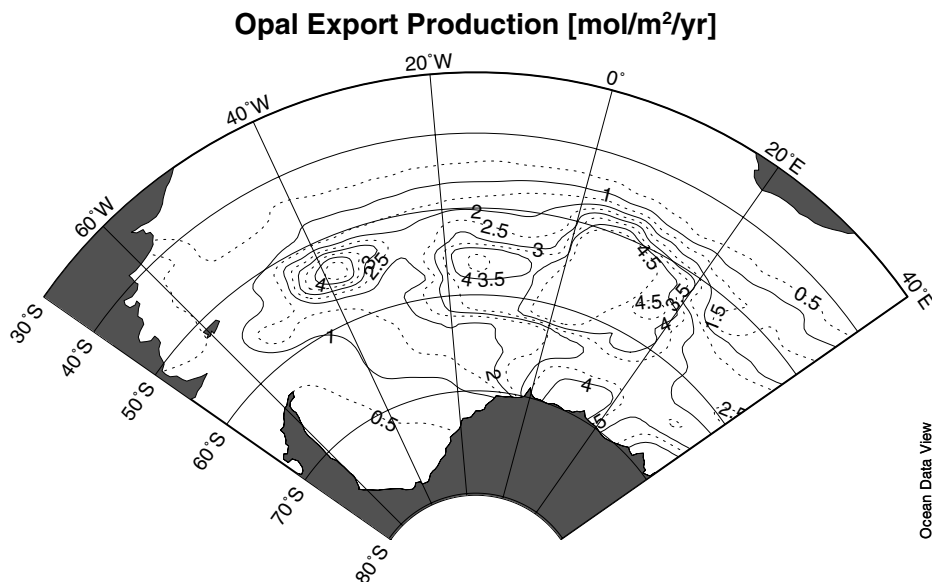


**Figure 11.** Annual opal export production at 133 m depth determined with the AAMOC model.

from nutrient data south of the Polar Front [Hoppe *et al.*, 2000]. In this area, strong upwelling is seen in the model solution that leads to enhanced silicate transports to the surface layer. Opal remineralization is moderate almost everywhere except south of 50°S and between 10°W and 30°E. Here the parameter  $b$  increases to values larger than 2; that is, opal is remineralized very rapidly below

133 m (Figure 12). The high export production of opal in the whole Weddell Gyre (except the almost year-round sea ice-covered region in the south west) is not mirrored in the fluxes to the seafloor apparently due to the rapid remineralization. High opal fluxes to the seafloor are only found in a latitudinal band at about 50°–55°S (Figure 13) north of the Weddell Gyre. These high fluxes give

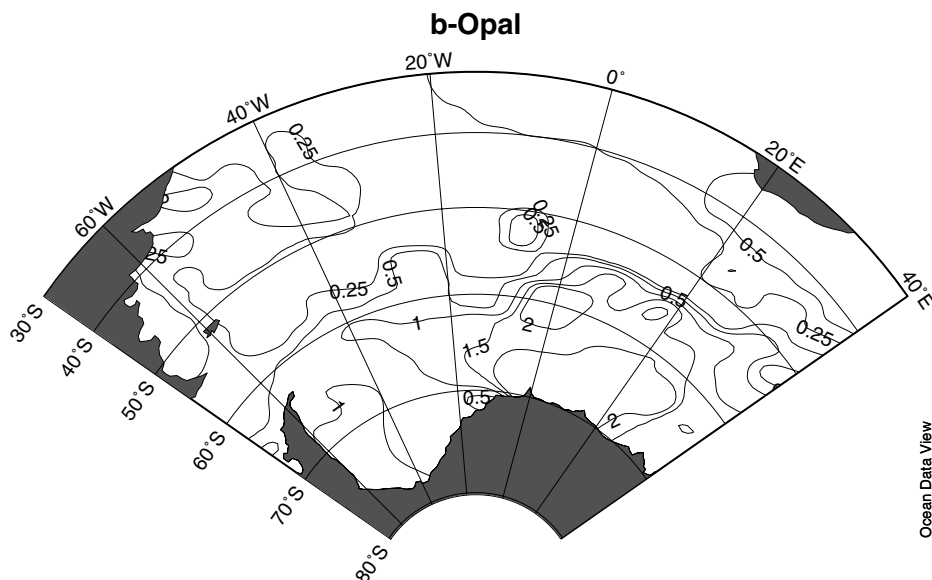


**Figure 12.** Opal remineralization depth scale  $b$  from AAMOC. Here  $b$  is the exponent in the Suess-type functions for particle flux  $a \cdot z^{-b}$ , where  $a$  is the export at 133 m depth (cf. Figure 11).

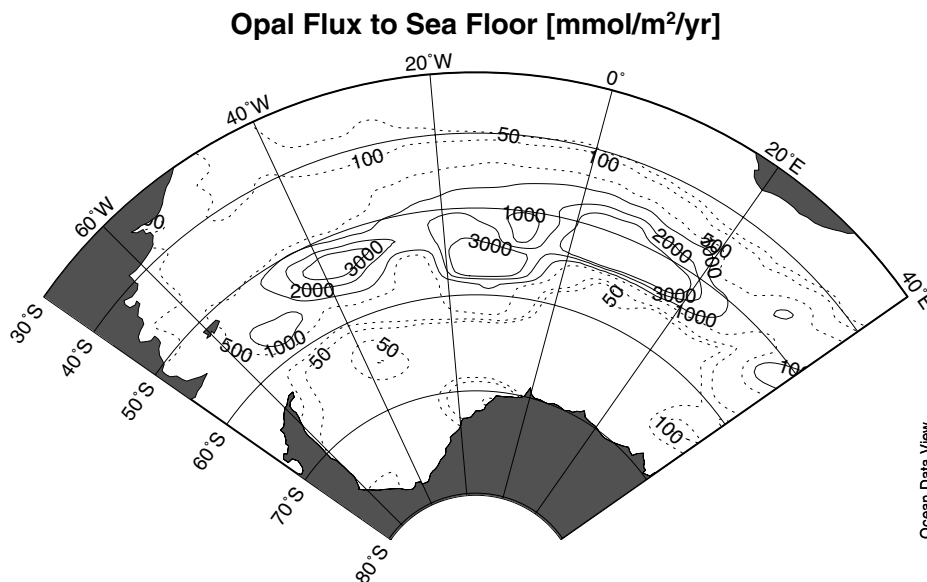


**Figure 13.** Opal flux to seafloor from AAMOCC. The flux to the seafloor is given by the flux to the bottom box. From this, a part is accumulated into the surface sediments; the rest is remineralized in the bottom box.

a similar pattern as the opal belt as drawn by *Lisitzin* [1996].

## 5. Discussion

### 5.1. Thorium-Based Export Fluxes

[18] The disequilibrium of  $^{234}\text{Th}$  with respect to its parent  $^{238}\text{U}$  is an accurate measure of the export of  $^{234}\text{Th}$  from the surface ocean and indirectly of other components of the particle flux like carbon and biogenic silica. We have studied the depletion of  $^{234}\text{Th}$  in surface waters around the Antarctic Polar Front on two previous expeditions to the area. In spring (ANT X/6 [*Bathmann et al.*, 1994]) we had observed the transition from a near-equilibrium distribution to a strong depletion (up to 38%) indicating an export event [*Rutgers van der Loeff et al.*, 1997], whereas in summer [*Bathmann et al.*, 1997a, 1997b; *M. M. Rutgers van der Loeff et al.*, Comparison of carbon and opal export rates between summer and spring bloom periods in the region of the Antarctic Polar Front, SE Atlantic, submitted to Deep Sea Research Part II, 2001], we observed a consistent depletion of 17% in the surface water and extending to a depth of 150–200 m. In both situations,  $^{234}\text{Th}$  was in equilibrium with  $^{238}\text{U}$  below 200 m. This means that the  $^{234}\text{Th}$  exported from the euphotic zone is distributed over a wide depth

interval or reaches the sediment. A  $^{234}\text{Th}$  excess below the euphotic zone has been reported only in very few occasions [*Coale and Bruland*, 1987]. An excess that balances the depletion in the surface water, leaving negligible export of  $^{234}\text{Th}$  beyond 350 m, as observed here in the open Weddell Sea, has not been observed before. Although it is conceivable that this distribution is a remnant of an earlier bloom (i.e., a few months before, e.g., during the seasonal retreat of the sea-ice), it is more likely that it is caused by a steady transport of fine material through the pycnocline and remineralization below.

[19] The  $^{234}\text{Th}$  data from the Weddell Sea show that a depletion in the surface water does not necessarily imply an export to depth. A transect of  $^{234}\text{Th}$  in surface waters, as given here in Figure 5, is clearly not sufficient to derive a geographical distribution of export fluxes as given in Figure 7. This situation is analogous to the chlorophyll distributions that cannot be safely derived from satellite data alone, as these are limited to the chlorophyll-a content in surface waters [*Antoine et al.*, 1996; *Behrenfeld and Falkowski*, 1997].

### 5.2. Inverse Modeling

[20] Inverse modeling of ocean circulation and biogeochemical fluxes based on reported distribu-

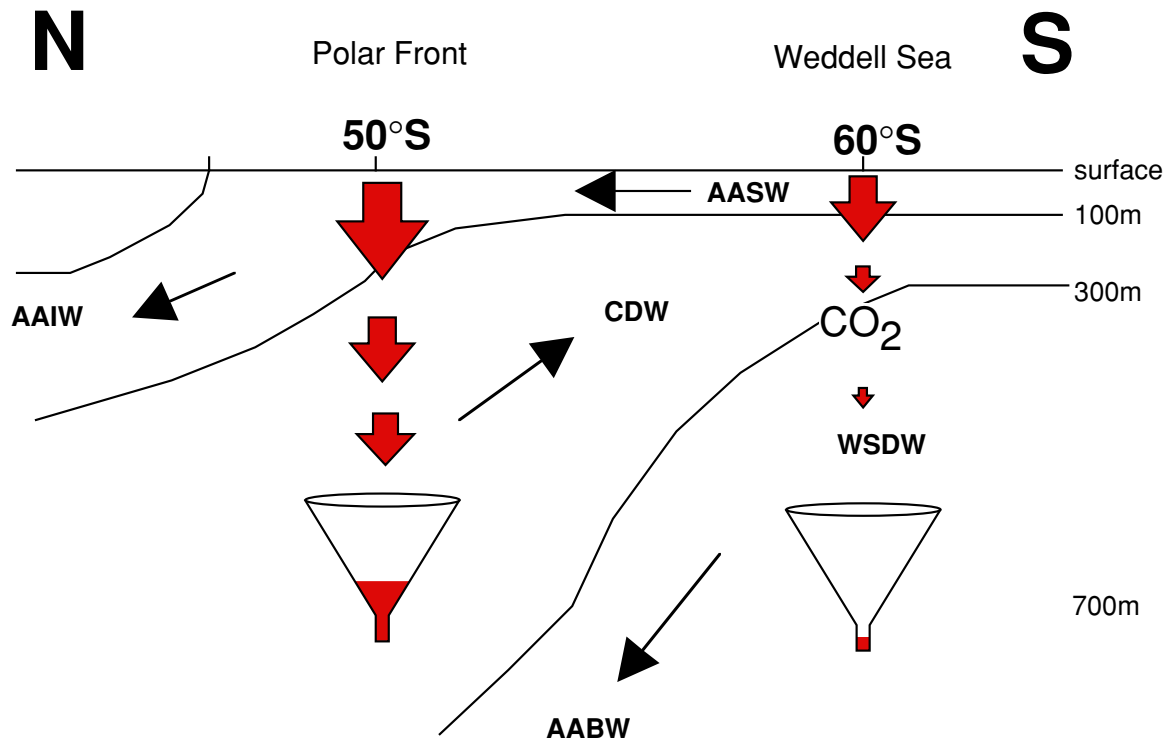


**Figure 14.** A conceptual model of shallow water column remineralization in the Weddell Sea.

tions of  $T$ ,  $S$ , and nutrients [Schlitzer, 2000, 2001; Usbeck, 1999; R. Usbeck et al., Particle fluxes in the ocean: Comparison of sediment trap data with results from inverse modeling, submitted to *Global Biogeochemical Cycles*, 2001] suggests shallow remineralization of organic material and biogenic silica in the Weddell Gyre and in addition gives a geographical distribution of the phenomenon. The results imply a high export production at 133 m of biogenic silica in the eastern Weddell Gyre (centered at 20°E, 60°S) that is rapidly dissolved in the water column beneath. A similar but less dramatic distribution was observed for the simulated organic carbon fluxes. High POC production and rapid remineralization is located further north and more closely associated with the fronts of the ACC. Recently Schlitzer [2001] showed that inclusion of labile dissolved organic carbon (DOC) in the model may have a considerable effect on export rates in the Southern Ocean. In his model experiments, part of the DOC produced in the surface water of the Southern Ocean is transported to depth during the formation of intermediate and bottom waters. As a

consequence, the export rates of particulate organic carbon are reduced in his model. In our present model we have not incorporated the production of DOC, as its actual production, export, and decay rates are still very uncertain. If in the Southern Ocean DOC plays the role suggested by Schlitzer, our POC export rates at 133 m and the remineralization rates would be somewhat overestimated. However, the overall contrast between high export rates and low flux rates at depth remains unchanged. Moreover, as the silica cycle is not considered to be influenced by a dissolved organic phase, the results of the export of biogenic silica are unaffected. It should be noted that the database of dissolved nutrients and silicate is relatively sparse in time and space south of 60°E and east of 10°E. However, the model incorporates a large part of the data available, and the combination of hydrographic constraints and nutrient budgets leads to the conclusion that in the Weddell Gyre a significant amount of nutrients is transported to middepth by vertical particle fluxes rather than due to advection/diffusion processes.

### 5.3. Proposed Explanation

[21] Although surface waters of the Weddell Sea have usually very low suspended particle loads and appear low in chlorophyll in satellite images, there is an appreciable export production from the upper ~200 m. Three lines of evidence, hydrographic features,  $^{234}\text{Th}$  export production, and inverse modeling, point to extremely shallow subsurface remineralization of particulate matter in the central Weddell Gyre. The export of particulate matter from the euphotic zone into subsurface waters causes nutrients and  $\text{CO}_2$  to increase in the Central Intermediate Water. Because the  $\text{CO}_2$ -enriched CIW is a permanent feature, this suggests that an equal amount is transported away laterally. This  $\text{CO}_2$  will be exported equatorward in deep and bottom waters, in which it is effectively isolated from contact with the atmosphere for a long time period (Figure 14).

[22] The residence time of particulate  $^{234}\text{Th}$  with respect to removal to the subsurface layer decreases to under one week in the central Weddell Sea (minimum 4.4 days based on data, stations at  $61^\circ$ – $67^\circ\text{S}$  in Figure 5), which is unusually short but not inconceivable. In addition to this surprisingly efficient transport out of the euphotic zone, there is an equally surprisingly efficient remineralization of biogenic detritus (POC and opal) in the subsurface layer right underneath the surface layer (cf. Figure 9 and Figure 12). We do not know what process is responsible for this transport at extremely low suspended particle loads and can only speculate on the possible role of particle composition and vertically migrating zooplankton.

[23] There are many possible mechanisms that may contribute to the observed shallow remineralization. The following combination of factors may be important with regard to our observations. In the region iron scarcity is prevalent, while iron limits phytoplankton growth [De Baar *et al.*, 1995]. This produces only a small biomass accumulation in the first place. Owing to this iron scarcity, predominantly smaller phytoplankton grows in these regions because they are more economic with the scarce iron [Detmer and Bathmann, 1997; Becquevort, 1997]. Small diatoms and siliceous nano-

plankton have been found to be relatively more abundant in the Weddell Gyre than near the Polar Front [Kozlova, 1966; Silver *et al.*, 1980; Klaas, 1997]. Small phytoplankton bears a proportionally larger surface area and, when inanimate, sinks slower than larger phytoplankton. It has been shown that the zooplankton in the Weddell Sea is dominated by copepods [Pakhomov *et al.*, 2000], which produce rapidly dissolving fecal pellets [Urban-Rich, 1999; Daly, 1997]. Also, salps (*Salpa Thompsoni*) widely occur in this region, and their ingestion rates are so high that they could account for 100% of the primary produced material [Dubischar and Bathmann, 1997]. Salps are known to produce fecal pellets with high sinking rates, but they can also produce rapidly disintegrating pseudo feces (U. Bathmann, personal communication, 2001). Several studies have been carried out to examine the role of secondary producers and carnivores for the carbon cycle, but the impact of grazers on the downward particle flux is not yet fully understood [Froneman *et al.*, 2000, and references therein]. However, diurnal vertical migration and subsequent remineralization at depth would be in good agreement with the extremely short timescale of shallow remineralization deduced from the  $^{234}\text{Th}$  results.

## 6. Conclusions

[24] The Weddell Sea, and perhaps larger areas of the High Nutrient Low Chlorophyll Southern Ocean, is characterized by highly efficient remineralization of biogenic detritus, organic carbon, and opal, at shallow depth (above 200 m). Indications for this have also been found in the Ross Sea [Nelson *et al.*, 1991; Smith and Dunbar, 1998; Gardner *et al.*, 2000], which thus suggests that this process may be widely occurring in the subpolar Southern Ocean. The subpolar region is the region south of the ACC, i.e., mainly Weddell Sea and Ross Sea.

[25] The annual export production of the surface layer of the central Weddell Gyre has been estimated to be around  $20 \text{ g Cm}^{-2}\text{yr}^{-1}$  [Hoppema *et al.*, 1999, 2001]. Such a figure indeed suggests that the export production is not that low. Since most of this will be remineralized in the subsurface water

column, as evidenced by the  $^{234}\text{Th}$  distribution, this is also the amount of carbon that is annually added to the CIW (cf. Figure 2). This mechanism essentially describes the operation of the biological pump of the central Weddell Sea. Provided the depth horizon of remineralization stays at constant depth, this is a steady state process which tends to reduce the partial pressure of  $\text{CO}_2$  in the surface layer, and part of the decay products including  $\text{CO}_2$  are transported to abyssal depth. However,  $\text{CO}_2$  released in the remineralization process is in part returned to the surface water by entrainment of subsurface water in the upwelling regime. The upwelling velocity in the central Weddell Sea is 30–45 m/yr [Gordon and Huber, 1990; Hoppema *et al.*, 1999]; the age of the surface layer with respect to upwelling is 2.5–3 years. Thus a substantial amount of remineralized  $\text{CO}_2$  is brought back into the surface layer. This additional  $\text{CO}_2$  tends to elevate the partial pressure of  $\text{CO}_2$  in the surface layer. Whether the Weddell Sea is a source or a sink for  $\text{CO}_2$  depends on the competition of the biological pump and the upwelling of  $\text{CO}_2$ -rich water from the CDW. Data of Hoppema *et al.* [1999] indicate that at present, the Weddell Gyre takes up atmospheric  $\text{CO}_2$ , but it is evident that the combined shallow remineralization and upwelling is a significant contribution to enhancing the  $\text{CO}_2$  in the surface layer of the Weddell Sea.

[26] A change of the environmental conditions either in the past or in the future could have strong impact on the competition of the shallow remineralization and the upwelling of  $\text{CO}_2$ -enriched subsurface waters. An even further shallowing of the effective remineralization horizon would enhance a tendency for  $\text{CO}_2$  increase of the Weddell Sea surface layer, but a deepening would promote the decrease of surface layer  $\text{CO}_2$ .

[27] No record of this productivity and associated export flux is stored in the sediment, and also estimates from satellite data lead to the conclusion of a “marine desert” in the Weddell Gyre. The amount of nutrients and  $\text{CO}_2$  recycled in the upper 500 m of the water column cannot be obtained from satellite data or the sedimentary record but might be of significance for global carbon budgets and also for the reconstruction of paleoproductivity.

## Acknowledgments

[28] We would like to thank Walter Geibert for fruitful discussions during the course of this study and preparation of the manuscript. We also like to thank two unknown reviewers for critically reading the manuscript and providing valuable comments. This work was supported by the EC Environment and Climate Research Programme (contract: ENV4-CT97-0472, Climate and Natural Hazards).

## References

- Anderson, R. F., N. Kumar, R. A. Mortlock, P. N. Froelich, P. Kubik, B. Dittrich-Hannen, and M. Suter, Late-Quaternary changes in productivity of the Southern Ocean, *J. Mar. Syst.*, **17**, 497–514, 1998.
- Antoine, D., J.-M. André, and A. Morel, Oceanic primary production, 2, Estimation at global scale from satellite (coastal zone color scanner) chlorophyll, *Global Biogeochem. Cycles*, **10**, 57–69, 1996.
- Bathmann, U. V., V. Smetacek, H. de Baar, E. Fahrbach, and G. Krause (Eds.), *The expeditions Antarktis X/6-8 of the research vessel Polarstern in 1992/93*, Rep. on Polar Res., **135**, Alfred Wegener Inst., Bremerhaven, 1994.
- Bathmann, U. V., M. Lucas, and V. Smetacek (Eds.), *The expeditions Antarktis XIII/1-2 of the research vessel Polarstern 1995/96*, Rep. on Polar Res., **221**, Alfred Wegener Inst., Bremerhaven, 1997a.
- Bathmann, U. V., R. Scharek, C. Klaas, C. D. Dubischar, and V. Smetacek, Spring development of phytoplankton biomass and composition in major water masses of the Atlantic sector of the Southern Ocean, *Deep Sea Res. Part II*, **44**, 51–67, 1997b.
- Bathmann, U., V. Smetacek, and M. Reinke, *The expeditions ANTARKTIS XVI/3-4 of the Research Vessel Polarstern 1999*, Rep. on Polar Res., **364**, Alfred Wegener Inst., Bremerhaven, 2000.
- Beckmann, A., H. H. Hellmer, and R. Timmermann, A numerical model of the Weddell Sea: Large-scale circulation and water mass distribution, *J. Geophys. Res.*, **104**, 375–391, 1999.
- Becquevort, S., Nanoprotozooplankton in the Atlantic sector of the Southern Ocean during early spring: biomass and feeding activities, *Deep Sea Res. Part II*, **44**, 355–373, 1997.
- Behrenfeld, M. J., and P. G. Falkowski, Photosynthetic rates derived from satellite-based chlorophyll concentration, *Limnol. Oceanogr.*, **42**, 1–20, 1997.
- Benitez-Nelson, C., K. O. Buesseler, M. M. Rutgers van der Loeff, J. Andrews, L. Ball, G. Crossin, and M. A. Charette, Testing a new small-volume technique for determining thorium-234 in seawater, *J. Radioanal. Nucl. Chem.*, **248**, 795–799, 2001.
- Berger, W. H., Appendix global maps of ocean productivity, in *Productivity of the Ocean: Present and Past, Dahlem Workshop Rep.*, edited by W. H. Berger, V. Smetacek, and G. Wefer, vol. 44, pp. 429–455, John Wiley, New York, 1989.
- Buesseler, K. O., M. P. Bacon, J. K. Cochran, and H. D. Livingston, Carbon and nitrogen export during the JGOFS

- North Atlantic bloom experiment estimated from  $^{234}\text{Th}$ :  $^{238}\text{U}$  disequilibria, *Deep Sea Res.*, *39*, 1115–1137, 1992.
- Coale, K. H., and K. W. Bruland, Oceanic stratified euphotic zone as elucidated by  $^{234}\text{Th}$ :  $^{238}\text{U}$  disequilibria, *Limnol. Oceanogr.*, *32*, 189–200, 1987.
- Daly, K. L., Flux of particulate matter through copepods in the Northeast Water Polynya, *J. Mar. Syst.*, *10*, 319–342, 1997.
- Deacon, G. E. R., The Weddell Gyre, *Deep Sea Res.*, *26*, 981–995, 1979.
- De Baar, H. J. W., J. T. M. de Jong, D. C. E. Bakker, B. M. Loescher, C. Veth, U. V. Bathmann, and V. Smetacek, Importance of iron for plankton blooms and carbon dioxide drawdown in the southern ocean, *Nature*, *373*, 412–415, 1995.
- de las Heras, M., and R. Schlitzer, On the importance of intermediate water flows for the global ocean overturning, *J. Geophys. Res.*, *104*, 15,515–15,536, 1999.
- DeMaster, D. J., The supply and accumulation of silica in the marine environment, *Geochim. Cosmochim. Acta*, *45*, 1715–1732, 1981.
- Detmer, A. E., and U. V. Bathmann, Distribution patterns of autotrophic pico- and nanoplankton and their relative contribution to algal biomass during spring in the Atlantic sector of the Southern Ocean, *Deep Sea Res. Part II*, *44*, 299–320, 1997.
- Dubischar, C. D., and U. V. Bathmann, Grazing impact of copepods and salps on phytoplankton in the Atlantic sector of the Southern Ocean, *Deep Sea Res. Part II*, *44*, 415–433, 1997.
- Fahrbach, E., G. Rohardt, M. Schröder, and V. Strass, Transport and structure of the Weddell Gyre, *Annal. Geophys.*, *12*, 840–855, 1994.
- Fischer, G., D. Fütterer, R. Gersonde, S. Honjo, D. Ostermann, and G. Wefer, Seasonal variability of particle flux in the Weddell Sea and its relation to ice cover, *Nature*, *335*, 426–428, 1988.
- Francois, R., M. A. Altabet, E. F. Yu, D. M. Sigman, M. P. Bacon, M. Frank, G. Bohrmann, G. Bareille, and L. D. Labeyrie, Organic carbon fluxes in the Atlantic and the Southern Ocean: relationship to primary production compiled from satellite radiometer data, *Nature*, *389*, 929–935, 1997.
- Froneman, P. W., E. A. Pakhomov, R. Perissinotto, and C. D. McQuaid, Zooplankton structure and grazing in the Atlantic sector of the Southern Ocean in late austral summer 1993, Part 2, Biogeochemical zonation, *Deep Sea Res. Part I*, *47*, 1687–1702, 2000.
- Gardner, W. D., M. J. Richardson, and W. O. Smith, Seasonal patterns of water column particulate organic carbon and fluxes in the Ross Sea, Antarctica, *Deep Sea Res. Part II*, *47*, 3423–3449, 2000.
- Geibert, W., *Actinium-227 als Tracer für Advektion und Mischung in der Tiefsee*, Rep. on Polar Res., *385*, Alfred Wegener Inst., Bremerhaven, 2001. (Available at <http://www.awi-bremerhaven.de/GEO/Publ/PhDs/Wgeibert>)
- Gordon, A. L., and B. A. Huber, Southern ocean winter mixed layer, *J. Geophys. Res.*, *95*, 655–672, 1990.
- Hoppema, M., E. Fahrbach, and M. Schröder, On the total carbon dioxide and oxygen signature of the Circumpolar Deep Water in the Weddell Gyre, *Oceanol. Acta*, *20*, 783–798, 1997.
- Hoppema, M., E. Fahrbach, M. H. C. Stoll, and H. J. W. de Baar, Annual uptake of atmospheric  $\text{CO}_2$  by the Weddell Sea derived from a surface layer balance, including estimations of entrainment and new production, *J. Mar. Syst.*, *19*, 219–233, 1999.
- Hoppema, M., E. Fahrbach, and H. J. W. de Baar, Surface layer balance of the southern Antarctic Circumpolar Current (prime meridian) used to derive carbon and silicate consumptions and annual air-sea exchange for  $\text{CO}_2$  and oxygen, *J. Geophys. Res.*, *105*, 11,359–11,371, 2000.
- Hoppema, M., H. J. W. de Baar, R. G. J. Bellerby, E. Fahrbach, and K. Bakker, Annual export production in the interior Weddell Gyre estimated from a chemical mass balance of nutrients, *Deep Sea Res. Part II*, in press, 2001.
- Jahnke, R. A., The global ocean flux of particulate organic carbon: Areal distribution and magnitude, *Global Biogeochem. Cycles*, *10*, 71–88, 1996.
- Kozlova, O. G., Diatoms of the Indian and Pacific Sectors of the Antarctic, Tech. Rep., Israel program for scientific translations, Jerusalem, Natl. Sci. Foundation, Washington, D.C., 1966.
- Klaas, C., Microprotozooplankton distribution and their potential grazing impact in the Antarctic Circumpolar Current, *Deep Sea Res. Part II*, *44*, 375–393, 1997.
- Leynaert, A., P. Tréguer, B. Quéguiner, and J. Morvan, The distribution of biogenic silica and the composition of particulate organic matter in the Weddell-Scotia Sea during summer 1988, *Mar. Chem.*, *35*, 435–447, 1991.
- Leynaert, A., D. M. Nelson, B. Quéguiner, and P. Tréguer, The silica cycle in the Antarctic Ocean: Is the Weddell Sea atypical?, *Mar. Ecol. Prog. Ser.*, *96*, 1–15, 1993.
- Lisitzin, A. P., *Oceanic Sedimentation: Lithology and Geochemistry*, AGU, Washington, D.C., 1996.
- Martin, J. H., and R. M. Gordon, Northeast Pacific iron distributions in relation to phytoplankton productivity, *Deep Sea Res.*, *35*, 177–196, 1988.
- Najjar, R. G., J. L. Sarmiento, and J. R. Toggweiler, Downward transport and fate of organic matter in the ocean: Simulations with a general circulation model, *Global Biogeochem. Cycles*, *6*, 45–76, 1992.
- Nelson, D. M., J. A. Ahern, and L. J. Herlihy, Cycling of biogenic silica within the upper water column of the Ross Sea, *Mar. Chem.*, *35*, 461–476, 1991.
- Nelson, D. M., P. Tréguer, M. A. Brzezinski, A. Leynaert, and B. Quéguiner, Production and Dissolution of biogenic silica in the ocean: Revised global estimates, comparison with regional data and relationship to biogenic sedimentation, *Global Biogeochem. Cycles*, *9*, 359–372, 1995.
- Orsi, A. H., W. D. Nowlin, and T. Whitworth, On the circulation and stratification of the Weddell Gyre, *Deep Sea Res. Part I*, *40*, 169–203, 1993.
- Orsi, A. H., T. Whitworth, and W. D. Nowlin, On the meridional extent and fronts of the Antarctic Circumpolar Current, *Deep Sea Res. Part I*, *42*, 641–673, 1995.
- Pakhomov, E. A., R. Perissinotto, C. D. McQuaid, and P. W. Froneman, Zooplankton structure and grazing in the Atlantic

- sector of the Southern Ocean in late austral summer 1993, Part 1, Ecological zonation, *Deep Sea Res. Part I*, 47, 1663–1686, 2000.
- Pondaven, P., O. Ragueneau, P. Tréguer, A. Hauvespre, L. Dezileau, and J. L. Reyss, Resolving the ‘opal paradox’ in the Southern Ocean, *Nature*, 405, 168–169, 2000.
- Redfield, A. C., B. C. Ketchum, and F. A. Richards, The influence of organisms on the composition of sea water, in *The Sea*, vol. 2, edited N. Hill, pp. 224–228, Interscience, New York, 1963.
- Rutgers van der Loeff, M. M., and G. W. Berger, Scavenging of  $^{230}\text{Th}$  and  $^{231}\text{Pa}$  near the Antarctic Polar Front in the South Atlantic, *Deep Sea Res. Part I*, 40, 339–357, 1993.
- Rutgers van der Loeff, M. M., J. Friedrich, and U. V. Bathmann, Carbon export during the spring bloom at the Antarctic Polar Front, determined with the natural tracer  $^{234}\text{Th}$ , *Deep Sea Res. Part II*, 44, 457–478, 1997.
- Rutgers van der Loeff, M. M., and W. S. Moore, 1999. Determination of natural radioactive tracers, in *Methods of Seawater Analysis*, 3rd edition, chap. 13 edited by K. Grasshoff, M. Ehrhardt, and K. Kremling, pp. 365–397, Verlag Chemie, Weinheim, Germany.
- Sarmiento, J. L., and J. R. Toggweiler, Downward transport and fate of organic matter in the ocean: Simulations with a general circulation model, *Global Biogeochem. Cycles*, 6, 45–76, 1992.
- Schlitzer, R., Determining the mean, large-scale circulation of the Atlantic with the adjoint method, *J. Phys. Oceanogr.*, 23, 1935–1952, 1993.
- Schlitzer, R., *An adjoint method for the determination of the mean oceanic circulation, air-sea fluxes and mixing coefficients*, Rep. on Polar Res., 156, Alfred Wegener Inst., Bremerhaven, 1995.
- Schlitzer, R., Applying the adjoint method for global biogeochemical modeling, in *Inverse Methods in Biogeochemical Cycles*, *Geophys. Monogr. Ser.*, vol. 114, edited by P. Kasibhatla, M. Heimann, D. Hartley, N. Mahowald, R. Prinn and P. Rayner, pp. 107–124, AGU, Washington, D.C., 2000.
- Schlitzer, R., Carbon export fluxes in the Southern Ocean: Results from inverse modeling and comparison with satellite based estimates, *Deep Sea Res. Part II*, in press, 2001.
- Schlüter, M., M. M. Rutgers van der Loeff, O. Holby, and G. Kuhn, Silica Cycle in Surface Sediments of the South Atlantic, *Deep Sea Res. Part II*, 45, 1085–1109, 1998.
- Schröder, M., and E. Fahrbach, On the structure and the transport of the eastern Weddell Gyre, *Deep Sea Res. Part II*, 46, 501–527, 1999.
- Silver, M. W., J. G. Mitchell, and D. L. Ringo, Siliceous nanoplankton, II, Newly discovered cysts and abundant choanoflagellates from the Weddell Sea, Antarctica, *Mar. Biol.*, 58, 211–217, 1980.
- Smith, W. O., and R. B. Dunbar, The relationship between new production and vertical flux on the Ross Sea continental shelf, *J. Mar. Syst.*, 17, 445–457, 1998.
- Stephens, B. B., and R. F. Keeling, The influence of Antarctic sea ice on glacial-interglacial  $\text{CO}_2$  variations, *Nature*, 404, 171–174, 2000.
- Stoll, M. H. C., H. J. W. de Baar, M. Hoppema, and E. Fahrbach, New early winter  $\text{fCO}_2$  data reveal continuous uptake of  $\text{CO}_2$  by the Weddell Sea, *Tellus, Ser B*, 51B, 679–687, 1999.
- Suess, E., Particulate organic carbon flux in the ocean-surface productivity and oxygen utilization, *Nature*, 280, 260–263, 1980.
- Urban-Rich, J., Release of dissolved organic carbon from copepod fecal pellets in the Greenland Sea, *J. Exp. Mar. Biol. Ecol.*, 232, 107–124, 1999.
- Usbeck, R., *Modeling of marine biogeochemical cycles with an emphasis on vertical particle fluxes*, Rep. on Polar Res., 332, Alfred Wegener Inst., Bremerhaven, 1999. (Available at <http://www.awi-bremerhaven.de/GEO/Publ/PhDs/Rusbeck>)
- Veizer, J., Y. Godderis, and L. M. Francois, Evidence for decoupling of atmospheric  $\text{CO}_2$  and global climate during the Phanerozoic eon, *Nature*, 408, 698–701, 2000.
- Walter, H. J., M. M. Rutgers van der Loeff, H. Hölzen, and U. V. Bathmann, Reduced scavenging of  $^{230}\text{Th}$  in the Weddell Sea: Implications for paleoceanographic reconstructions in the South Atlantic, *Deep Sea Res. Part I*, 47, 1369–1387, 2000.
- Walter, H. J., W. Geibert, M. M. Rutgers van der Loeff, G. Fischer, and U. V. Bathmann, Shallow vs. deep-water scavenging of  $^{231}\text{Pa}$  and  $^{230}\text{Th}$  in radionuclide enriched waters of the Atlantic sector of the Southern Ocean, *Deep Sea Res. Part II*, 48, 471–493, 2001.
- Whitworth, T., and W. D. Nowlin, Water masses and currents of the Southern Ocean at the Greenwich Meridian, *J. Geophys. Res.*, 92, 6462–6476, 1987.
- Yamanaka, Y., and E. Tajika, The role of the vertical fluxes of particulate organic matter and calcite in the oceanic carbon cycle: Studies using an ocean biogeochemical general circulation model, *Global Biogeochem. Cycles*, 10, 361–382, 1996.
- Yamanaka, Y., and E. Tajika, Role of dissolved organic matter in the marine biogeochemical cycle: Studies using an ocean biogeochemical general circulation model, *Global Biogeochem. Cycles*, 11, 599–612, 1997.